Center for Modeling of Turbulence and Transition
Research Briefs - 1991

Modeling of Turbulent Shear Flows

William W. Liou

1. Motivation and Objective

This report documents the current progress in the research and development of modeling techniques for turbulent shear flows. These include a two-scale model for compressible turbulent flows and a new energy transfer model. The former represents the status of our efforts to identify compressibility effects in turbulence. The energy transfer model refines a weakly nonlinear wave model developed earlier, which models directly the turbulent large structures. The objective of these activities is to develop second-order closures for compressible turbulent flows.

2. Work Accomplished

2.1 A Two-Scale Model for Compressible Turbulent Flows

Numerical simulations of 2D and 3D compressible turbulence have shown that the existence of shocklet structures and the energy transfer mechanism between the kinetic energy and the thermal-energy are the two important compressibility effects[1,2,3,4]. These compressibility effects are incorporated into a new two-scale model. The model is based on the proposition that the effect of compressibility in turbulence is mainly on the energetic large eddies in turbulent shear flows. The small eddies are affected only indirectly through the increased spectral energy transfer. The development of the model and some results of its application to compressible free shear layers are briefly described here. A more detailed analysis is included in a NASA TM[5].

Firstly, it is assumed that the shocklet structures that may occur intermittently in compressible turbulent flows are formed mainly by the collision of the energetic turbulent eddies of large scale. The small eddies, which contain much less energy, are less efficient in the formation of shocklet structures when they collide with other eddies. Thus, the eddy shocklets scale with the energy containing eddies and have more direct influence on the evolution of the large eddies than on the smaller ones. The large vortical structures are intensified as they pass through the shocklet. This process, in other words, enhances the vortex stretching mechanism and increases the spectral energy transfer. In addition to the usual route of the vortex stretching mechanism that has already been enhanced, the small eddies may be generated directly from the passage of the large vortical structures through shock waves These processes of enhanced energy transfer may then cause the spectrum to depart from equilibrium. Another mechanism that may also contribute to the non-equilibrium spectrum or the creation of vorticity is strongly related to the pressure fluctuation. It has been shown by Kida and Orszag[3] and Lee *et al.*[2], among others, that substantial vorticity is created by the baroclinic terms. The creation of vorticity, however, occurs mainly at the shock wave.

Based on the picture described above, the effect of compressibility in turbulence is mainly on the energy containing large eddies or the low wavenumber fluctuations. The large eddies respond more readily to changes in the compressible mean flow resulting from either high speed or combustion. The straining of the large eddies due to compressibility effects increases the spectral energy transfer to the small scales through the mechanism of vortex stretching and direct generation. The smaller scales, on the other hand, are only indirectly affected by compressibility. The energy contained in the small scales in the high wavenumber part of the energy spectrum is increased only as more energy is pumped in from the large eddies associated with the low wavenumber part of the spectrum. To model the Favre-averaged mean compressible turbulent quantities associated with these two distinct regimes in the energy spectrum we solve the modeled transport equations for the kinetic energy of the large eddy (k_p) and the small eddy (k_t) and the rate of energy transfer from the large eddy to the small eddy (ϵ_p) and the rate of energy dissipation (ϵ_t). The transport equations are

$$\overline{\rho}\frac{\overline{\mathrm{D}}\widetilde{k_p}}{\overline{\mathrm{D}}t} = \frac{d}{dy}[(\overline{\mu}+\frac{\mu_T}{\sigma_{\widetilde{k_p}}})\frac{d\widetilde{k_p}}{dy}] + \mu_T(\frac{d\widetilde{u}}{dy})^2 - \overline{\rho}\widetilde{\epsilon_p} + \text{P.D.} \tag{1}$$

$$\overline{\rho}\frac{\overline{\mathrm{D}}\widetilde{\epsilon_p}}{\overline{\mathrm{D}}t} = \frac{d}{dy}[(\overline{\mu}+\frac{\mu_T}{\sigma_{\widetilde{\epsilon_p}}})\frac{d\widetilde{\epsilon_p}}{dy}] + Cp_1\frac{\widetilde{\epsilon_p}}{\widetilde{k_p}}\mu_T(\frac{d\widetilde{u}}{dy})^2 - Cp_2'\overline{\rho}\frac{\widetilde{\epsilon_p}^2}{\widetilde{k_p}} + \text{E.S.} \tag{2}$$

$$\overline{\rho}\frac{\overline{\mathrm{D}}\widetilde{k_t}}{\overline{\mathrm{D}}t} = \frac{d}{dy}[(\overline{\mu}+\frac{\mu_T}{\sigma_{\widetilde{k_t}}})\frac{d\widetilde{k_t}}{dy}] + \overline{\rho}\widetilde{\epsilon_p} - \overline{\rho}\widetilde{\epsilon_t} \tag{3}$$

$$\overline{\rho}\frac{\overline{\mathrm{D}}\widetilde{\epsilon_t}}{\overline{\mathrm{D}}t} = \frac{d}{dy}[(\overline{\mu}+\frac{\mu_T}{\sigma_{\widetilde{\epsilon_t}}})\frac{d\widetilde{\epsilon_t}}{dy}] + Ct_1\overline{\rho}\frac{\widetilde{\epsilon_t}\widetilde{\epsilon_p}}{\widetilde{k_t}} - Ct_2\overline{\rho}\frac{\widetilde{\epsilon_t}^2}{\widetilde{k_t}} \tag{4}$$

P.D. and E.S. denote the effects of pressure-dilatation and eddy shocklets, respectively. The definition of the model constants can be found in the NASA TM. The present two-scale model for compressible turbulence is built upon a parallel model for incompressible flows, Duncan *et al.*[6]. Models for the terms responsible for the compressibility effects are needed to close the equations. In this analysis, we have adopted Sarkar's[7] model for the pressure-dilatation terms. To model the effects of the increased spectral energy transfer due to compressibility, a simple model has been constructed through dimensional reasoning. Its coefficient has a M_t^2 dependence, similar to the dilatation dissipation model proposed by Zeman[8] and Sarkar *et al.*[9]. The compressibility corrections that they proposed have been implemented successfully into $k-\epsilon$ models, Viegas and Rubesin[10], into $k-\omega$ models, Wilcox[11] and into second-order closure models, Speziale and Sarkar[12].

Fig. 1 shows the variation of the vorticity thickness growth rate, $\mathrm{d}\delta_\omega/\mathrm{d}x$, as a function of convective Mach number. The vorticity thickness, δ_ω, is defined by

$$\delta_\omega = \frac{U_f - U_s}{(\mathrm{d}U/\mathrm{d}y)_{max}}. \tag{5}$$

The convective Mach number is defined as the ratio of the average convective velocity of the dominant large scale structures, relative to the free stream, to the free stream speeds of sound, Papamoschou and Roshko[13]. The convective Mach number has been shown to be an appropriate parameter to correlate experimental data and to identify the effects of compressibility. The vorticity thickness growth rates for compressible free shear flows, $(d\delta_\omega/dx)(M_c, U_s/U_f, \rho_s/\rho_f)$, have been normalized by the corresponding values for incompressible flows, $(d\delta_\omega/dx)_i(0, U_s/U_f, \rho_s/\rho_f)$, and are presented in Fig. 1. The value of $(d\delta_\omega/dx)_i$ is obtained by using a relation, Papamoschou and Roshko[13],

$$(\frac{d\delta_\omega}{dx})_i \sim \frac{(1-\frac{U_s}{U_f})(1+(\frac{\rho_s}{\rho_f})^{1/2})}{1+\frac{U_s}{U_f}(\frac{\rho_s}{\rho_f})^{1/2}}. \tag{6}$$

The constant of proportionality is obtained by the present model calculations performed in the limit of $M_c \to 0$. Measured data are denoted by open symbols in Fig. 1. Without the compressibility corrections, the current two-scale model and the two-scale model developed by Kim and Chen[14] (KC) predict a large reduction of the growth rate only at very high convective Mach numbers. With the inclusion of the effects of eddy shocklets and the pressure work, the current compressible two-scale model predicts a smooth reduction of the vorticity thickness growth rate as the convective Mach number increases. The calculated growth rate curve levels off at high convective Mach numbers. It should be noted that in the present analysis the convective Mach number of the shear layer is increased by increasing the Mach number of the high speed stream. According to the definition of the convective Mach number, there exists a maximum convective Mach number for a plane mixing layer of the same fluid with matched total temperature. That is,

$$\lim_{M_f \to \infty} M_c = \frac{1-r}{(\frac{(\gamma-1)(1-r^2)}{2})^{1/2}} \tag{7}$$

where $r = U_s/U_f$ and γ denotes the ratio of the specific heats of the working fluid. For a value of R=0.1, the limiting convective Mach number for a plane shear layer of air is about 2.0.

Since it is the Reynolds shear stress that appears in the mean momentum equations and influences directly the development of the mean flow, it is interesting to see how its peak value varies as a function of M_c. Note that in the current analysis, the Reynolds shear stress is related to the mean flow by a turbulent eddy viscosity, μ_t. That is,

$$-\bar{\rho}\widetilde{u'v'} = \mu_T \frac{\partial \tilde{u}}{\partial y} \tag{8}$$

and

$$\mu_T = C_\mu \bar{\rho} \frac{(\tilde{k_p}+\tilde{k_t})^2}{\tilde{\epsilon_p}} \tag{9}$$

In Fig. 2, the peak Reynolds shear stresses predicted by the present compressible two-scale model are compared with measured data, Elliott and Samimy[15]. The predictions of the present model, without compressibility corrections and of the KC model are also shown for comparison. The results show that, without the inclusion of some forms of compressibility corrections, none of the two-scale models tested, including the current model and the KC model, performs satisfactorily in the calculations of compressible free shear layers. The present compressible two-scale model under-predicts the absolute value of the peak Reynolds shear stress. However, the trend observed in the experiment that the level of the peak Reynolds shear stress decreases with increasing convective Mach number is picked up consistently by the current compressible two-scale model. Note that the Reynolds shear stress has been normalized by the square of the velocity difference of the two free streams. The model also shows that the value of the peak Reynolds shear stress appears to be independent of the velocity ratio of the free streams. In fact, the predicted variation of the peak value of the Reynolds shear stress as a function of the convective Mach number is similar to the predicted variation of the normalized vorticity thickness growth rate as a function of the convective Mach number. This characteristic of the present compressible two-scale model is consistent with the observation made by Elliott and Samimy[15]. They argue that, based on an integral analysis, the decreasing trend of the level of the Reynolds shear stress, as the convective Mach number is increased, is due mainly to the decrease of momentum thickness growth rate. However, the two speed ratios considered here, 0.1 and 0.2, are nearly equal to each other. Cases with a wider range of operating conditions, such as the speed ratios and the working fluids, need to be examined before any conclusive statement can be made.

To further validate the present compressible two-scale model, it is applied to the compressible free shear layer corresponding to the Case 1 in Samimy and Elliott[16]. In this case, a fully expanded plane shear layer of air with $M_c = 0.51$ and $r = 0.36$ is examined. The calculated mean profile shown in Fig. 3 agrees reasonably well with the measurement. As described previously, there are many possible causes for the small difference in the outer region of the mixing zone. Fig. 4 shows the comparison of the computed and the measured Reynolds shear stress. The present two-scale model under-predicts the peak Reynolds shear stress by about 12%. The profile of the Reynolds shear shear stress, however, agree very well with the measurement.

2.2 A New Energy Transfer Model for Turbulent Free Shear Flows

The model is built upon the weakly nonlinear wave models developed by Liou and Morris[17]. The development of the energy transfer model and some results of its application to an incompressible free shear layer are briefly described here. A more detailed analysis is included in a NASA TM[18].

The random flow properties are split into three components,

$$\tilde{f}_i = F_i + f_i + f_i' \qquad (10)$$

The fluctuation with respect to the long time-average component, F_i, is separated into a component representing the large-scale motion, f_i, and one representing

the residual fluctuations, f_i'. The long time-average of the instantaneous value is denoted by an overbar,

$$\bar{\tilde{f}}_i = F_i = \frac{1}{T_1}\int_0^{T_1} \tilde{f}_i \mathrm{d}t \tag{11}$$

For the large-scale fluctuation, a separable form of solution is assumed,

$$\{\mathbf{u},\ \mathbf{v},\ \mathbf{p}\} = A(x)\,[\hat{u}(y),\hat{v}(y),\hat{p}(y)]\ exp\ [i(\alpha x - \omega t)]. \tag{12}$$

The bold face quantities denote a complex solution whose real part describes the physical properties of the large-scale structures. $\alpha\ (=\alpha_r + i\alpha_i)$ denotes a complex wavenumber and ω the frequency. The governing equations for the local distributions of the large structures can be reduced to the Rayleigh equation in terms of $\hat{v}$,

$$\left\{(\alpha U - \omega)\left(\frac{\mathrm{d}^2}{\mathrm{d}y^2} - \alpha^2\right) - \alpha\frac{\mathrm{d}^2 U}{\mathrm{d}y^2}\right\}\hat{v} = 0 \tag{13}$$

The amplitude, $A(x)$, appears as a parameter in the local calculation for the $\hat{u},\hat{v},\hat{p}$ and is determined separately from the large scale turbulent kinetic energy equation,

$$U_j\frac{\partial k}{\partial x_j} = -\overline{u_i u_j}\frac{\partial U_i}{\partial x_j} - \frac{\partial}{\partial x_j}\left(\overline{u_j k} + \overline{\frac{pu_j}{\varrho}}\right) - \overline{(-<u_i' u_j'>)\frac{\partial u_i}{\partial x_j}}$$

$$- \frac{\partial}{\partial x_j}\overline{(u_i <u_i' u_j'>)} + \text{viscous terms} \tag{14}$$

where $k = \frac{1}{2}\overline{u_i u_i}$. k denotes the turbulent kinetic energy of the large-scale structure. Note that in this analysis k denotes the turbulent kinetic energy of large scale structure of a single mode. The $\widetilde{k}_p$ defined in the first part of this report represents the sum of the turbulent kinetic energy of all the modes in the entire large-scale spectrum. <> represents a short time-average with an average interval much smaller than T_1 but much larger than the characteristic time scale of the background small-scale fluctuation, Strange and Crighton[19]. The interaction terms, the third expression on the right hand side of equation (14), describe the transfer of large-scale energy, presumably, to the small scales where energy is eventually dissipated by viscosity. The detailed analysis of the weakly nonlinear wave models and the numerical solution procedure used here can be found in Liou and Morris[17].

The spectral energy transfer results from the interactions between turbulent fluctuations of different scales. For the weakly nonlinear wave turbulence models, the energy transfer is of crucial importance in the determination of the wave amplitude and needs to be considered carefully. Very little information, experimental or theoretical, is available regarding the stresses, $-<u_i' u_j'>$.

The weakly nonlinear analysis seeks normal mode solution of the large-scale turbulent fluctuation. Locally, the fluctuations are described by the linearized Euler

equations. On the other hand, the spatial extent of each of the modes of the large-scale structures could be regarded as being determined by the wavenumber, α_r. Therefore, the proposition here is to estimate the characteristic size of the large scales as the wavelength associated with the large structures, which are predicted by the weakly nonlinear analysis. That is,

$$l = l_w = \frac{2\pi}{\alpha_r}. \tag{15}$$

where l_w denotes the wavelength. Through dimensional reasoning, the enregy transfer can be modeled by

$$C_2 \frac{k^{\frac{3}{2}}}{l_w} \tag{16}$$

This is the proposed model for the energy transfer from the large scale to the small scale. This estimate is in accord with the classic assumption of turbulence theory that dissipation ".. proceeds at a rate dictated by the inviscid inertia behavior of the large eddies", Tennekes and Lumley [20]. Computationally, since the wavenumber is already a part of the solution of the equations for the large-scale fluctuation, this model involves no extra efforts in estimating the characteristic size of the energy containing large scales. This rather simple model provides a closure to the equations for the large-scale structure, thereby allowing render the weakly nonlinear wave description of the large-scale structure to be self-contained. This self-contained nature of the weakly nonlinear wave turbulence models may be important in the future applications to other turbulent free shear flows.

The model is tested against an incompressible plane mixing layer. Since the most unstable mode interacts most strongly with the mean flow[17], the most amplifying local instability is used in the modeling of the average, overall interactions between the mean and the large scale motions. Therefore, in the present formulation, the characteristic length scale l_w is determined only by the locally most unstable modes.

Fig. 5 shows the predicted evolution of the streamwise mean velocity profiles with axial distance. η is a similarity coordinate,

$$\eta = \frac{y - y_{1/2}}{x - x_0} \tag{17}$$

where $y_{1/2}$ denotes the location where the local mean velocity is one half of the free stream velocity. The predicted self-similar profiles agree well with that compiled by Patel[21] except at the low speed edge of the layer. Similar differences were also observed by Liou and Morris[17]. They attributed this difference to the single mode representation of the entire large scale spectrum and the uncertainties in the measurements in this region resulting from the local large changes in the instantaneous flow direction.

The streamwise evolution of the amplitude of the large-scale structures is shown in Fig. 6. After a region of establishment, the amplitude reaches a saturated value.

In this region, the rate of the production of the large-scale turbulent kinetic energy from the mean flow is balanced by the rate of energy transfer from the large scales to the small scales. Note that, for the present energy transfer model, the amplitude equation becomes,

$$\frac{\mathrm{d}A^2}{\mathrm{d}x} = G_3(x)\,A^2 - G_4(x)\,A^3 \tag{18}$$

G_3 and G_4 denote the normalized positive definite integrals of the production terms and interaction terms across the layer, respectively. The critical points of the nonlinear equation (18), where $\mathrm{d}A^2/\mathrm{d}x = 0$, are $A_1 = 0$ and $G_4(x_2)A_2 = G_3(x_2)$. Simple analyses by applying the Liapunov function method[22] show that A_1 is an unstable critical point. Any small disturbances to A_1, say A_1' would grow exponentially. In fact,

$$(A_1^2)' \approx e^{G_3(x_1)\,x} \tag{19}$$

A_2, on the other hand, is asymptotically stable. A disturbance about the A_2, say A_2', would decay exponentially,

$$(A_2^2)' \approx e^{-\frac{G_3(x_2)}{2}\,x} \tag{20}$$

The saturated value of the amplitude, A_2, is an asymptotically equilibrium value. It indicates an asymptotically equilibrium state of the large-scale structures. The simple instability analyses also show that any deviation away from this equilibrium state would be damped out exponentially. Consequently, the saturation of the wave amplitude may provide an indication of the the self-similarity of the flow in terms of the development of the large-scale structures.

3. Future Plans

3.1 A Two-Scale Model for Compressible Turbulent Flows

(1) Extend the two-scale model to wall-bounded flows.

(2) Continue the development of second-order closure models that account explicitly for the compressibility effects identified during the development of the two-scale eddy-viscosity model.

3.2 A New Energy Transfer Model for Turbulent Free Shear Flows

(1) Apply the weakly nonlinear wave model to compressible mixing layers to investigate the effects of compressibility on the characteristics of the coherent large-scale structures.

4. References

[1] Passot, T. and Pouquet, A., "Numerical simulation of compressible homogeneous flows in the turbulent regime," J. Fluid Mech., **181**, 441-466 (1987).

[2] Lee, S., Lele, S. K. and Moin, P., "Direct numerical simulation and analysis of shock turbulence interaction," AIAA paper 91-0523.

[3] Kida, S. and Orszag, S. A., "Energy and spectral dynamics in forced compressible turbulence," J. Sci. Comp. **5** (1990).

[4] Kida, S. and Orszag, S. A., "Enstrophy budget in decaying compressible turbulence," J. Sci. Comp. (1991)

[5] Liou, W. W. and Shih, T.-H., "A two-scale model for compressible turbulent flows," NASA TM (to appear) (1992).

[6] Duncan, B. S., Liou, W. W. and Shih, T.-H., "A Multiple-scale turbulence model for incompressible flow," NASA TM (to appear) (1992).

[7] Sarkar, S., Erlebacher, G., Hussaini, M. Y. and Kreiss, H. O., " The analysis and modeling of dilatational terms in compressible turbulence," NASA CR 18195 (1989).

[8] Zeman, O., "Dilatation dissipation: The concept and application in modeling compressible mixing layers," Phys. Fluids A **2** (2), 178-188 (1990).

[9] Sarkar, S., Erlebacher, G. and Hussaini, M. Y., "Compressible homogeneous shear: simulation and modeling," NASA CR 189611 (1992).

[10] Viegas, J. R. and Rubesin, M. W., "A comparative study of several compressibility corrections to turbulence models applied to high-speed shear layers," AIAA paper 91-1783.

[11] Wilcox, D. C., "Progress in hypersonic turbulence modeling," AIAA paper 91-1785.

[12] Speziale, C. G. and Sarkar, S., "Second-order closure models for supersonic turbulent flows," AIAA paper 91-0217.

[13] Papamoschou, D. and Roshko, A., "The compressible turbulent shear layer: an experimental study," J. Fluid Mech. **197**, 453-477 (1988).

[14] Kim, S.-W. and Chen, C.-P., "A multiple-time-scale turbulence model based on variable partitioning of turbulent kinetic energy spectrum," NASA CR-179222 (1987).

[15] Elliott, G. S. and Samimy, M., "Compressibility effects in free shear layers," Phys. Fluids A (1991)

[16] Samimy, M. and Elliott, G. S., "Effects of compressibility on the characteristics of free shear layers," Phys. Fluids A **28**, 439-445 (1990).

[17] Liou, W. W. and Morris, P. J., "Weakly nonlinear models for turbulent mixing in a plane mixing layer," to appear in Phys. Fluids (1992).

[18] Liou, W. W., "A new energy transfer model for turbulent free shear flows," NASA TM (to appear) (1992).

[19] Strange, P. J. R. and Crighton, D. G., "Spinning modes on axisymmetric jets, Part I," J. Fluid Mech. **134**, 231-245 (1983).

[20] Tennekes, H. and Lumley, J. L., *A First Course in Turbulence*, M.I.T. Press, 1972.

[21] Patel, R. P., "An experimental study of a plane mixing layer," AIAA Journal **11**, 67-71 (1973).

[22] Simmons, G. F., *Differential Equations with Applications and Historical Notes*, McGraw Hill, 1972.

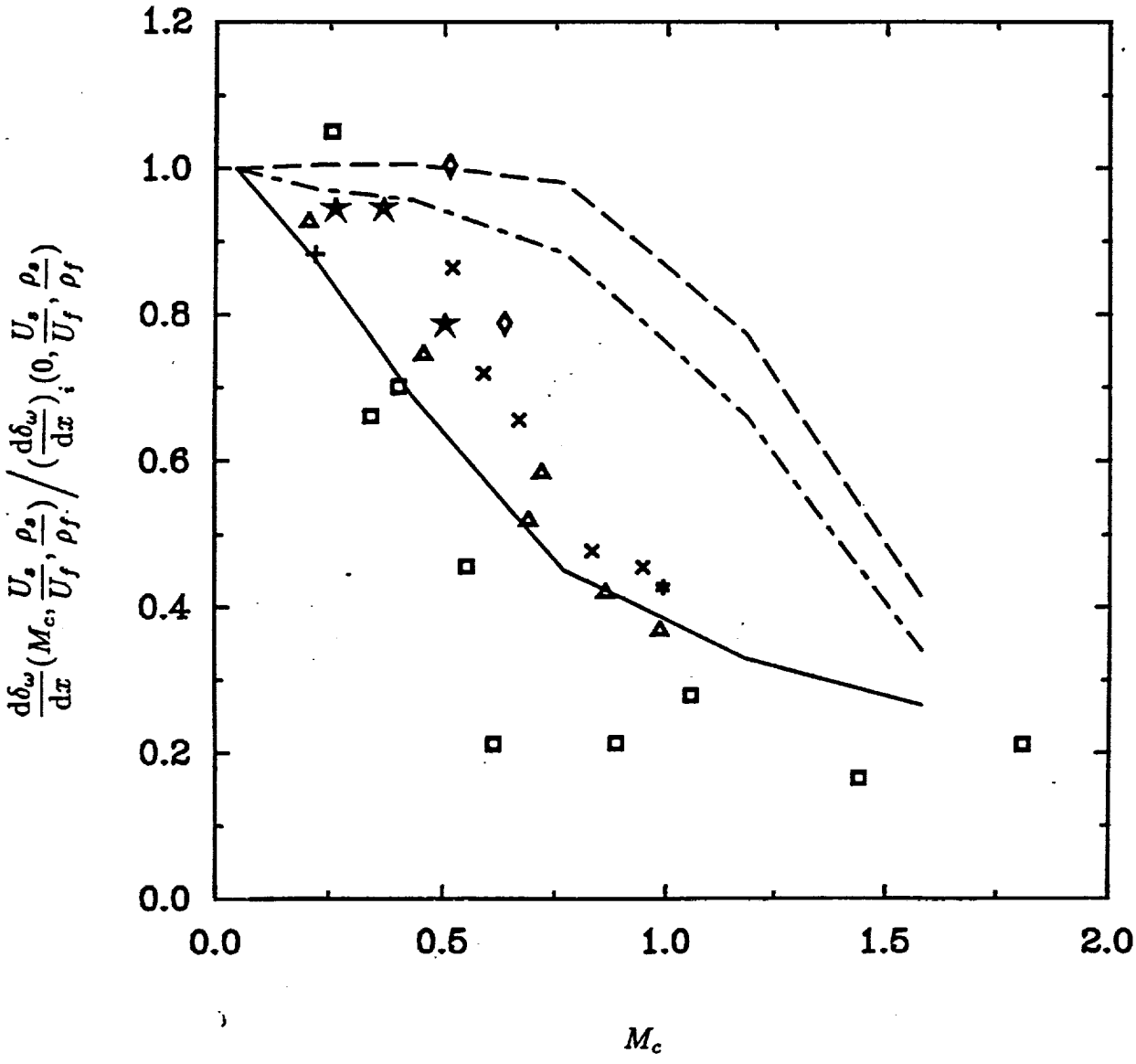

Figure 1. Variation of relative growth rate with convective Mach number, $r = 0.1$. — —, Present: without compressibility corrections; ——— , Present: with compressibility corrections; – ——, KC; □ , Papamoschou and Roshko; △ , Goebel *et al* ; ◇ , Samimy and Elliott; ★ , Sullins *et al*; + , Messersmith *et al*; × , Chinzei *et al*; ✱ , Ikawa and Kubota *et al.*

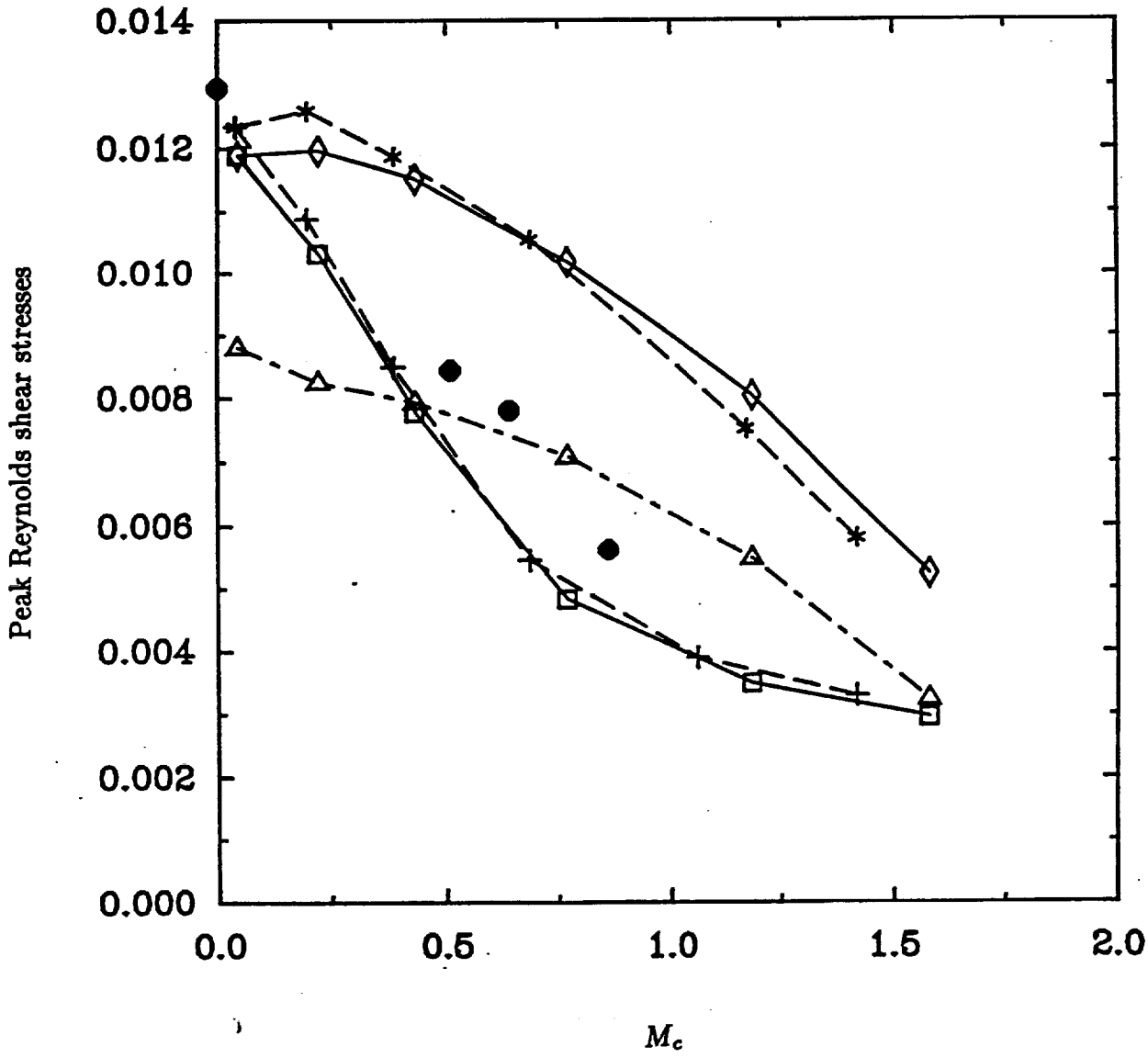

Figure 2. Variation of the peak Reynolds shear stress with convective Mach number. —◇—, Present: $\tau = 0.1$, without compressibility corrections; —□—, Present: $\tau = 0.1$, with compressibility corrections;— * —, Present: $\tau = 0.2$, without compressibility corrections;— + —, Present: $\tau = 0.2$, with compressibility corrections;– ——, KC: $\tau = 0.1$; ●, Elliott and Samimy.

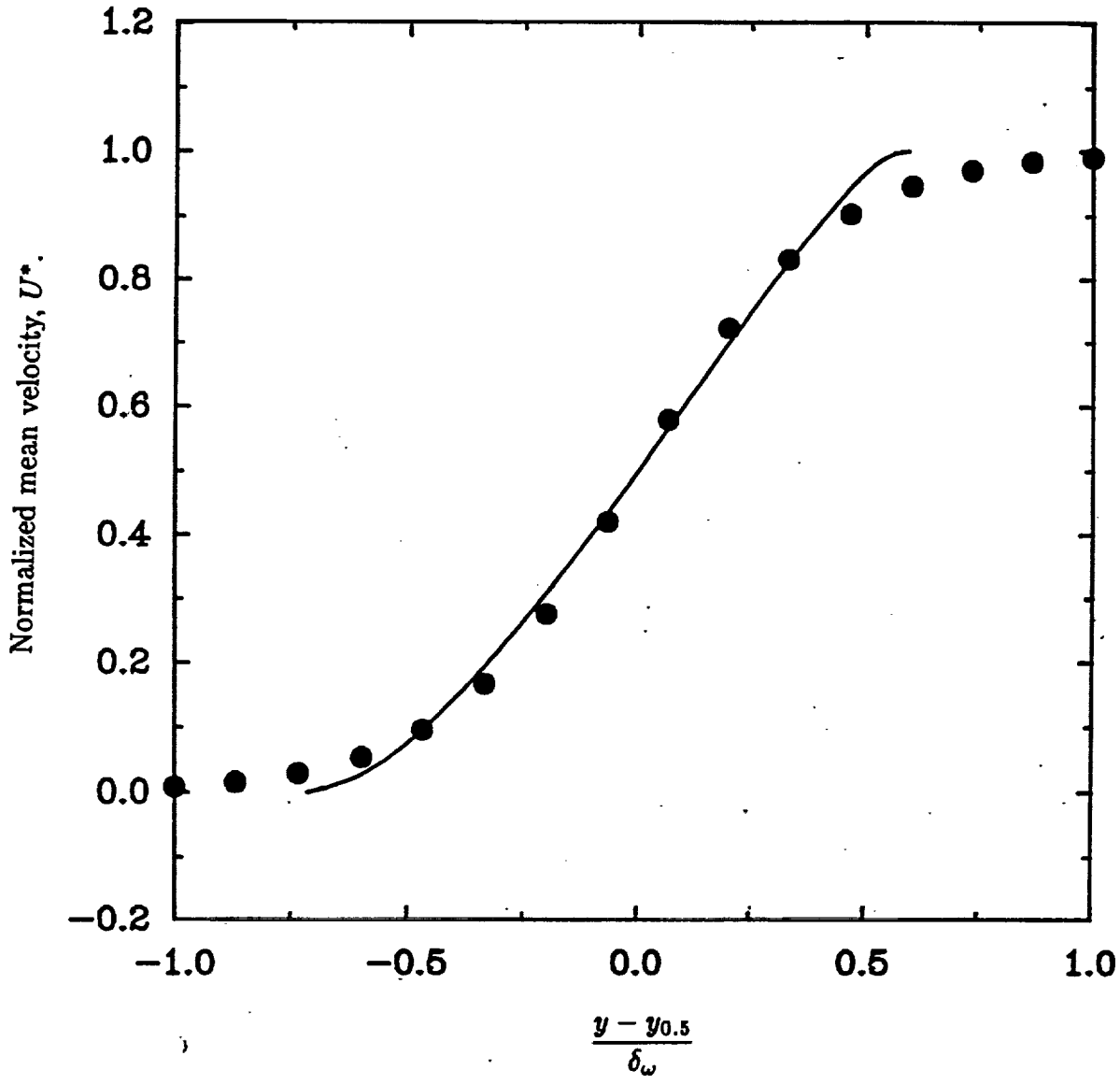

Figure 3. Comparison of mean velocity profiles for the shear layer in Case 1 of Elliott and Samimy (1991). ——, Present; ● , experiment.

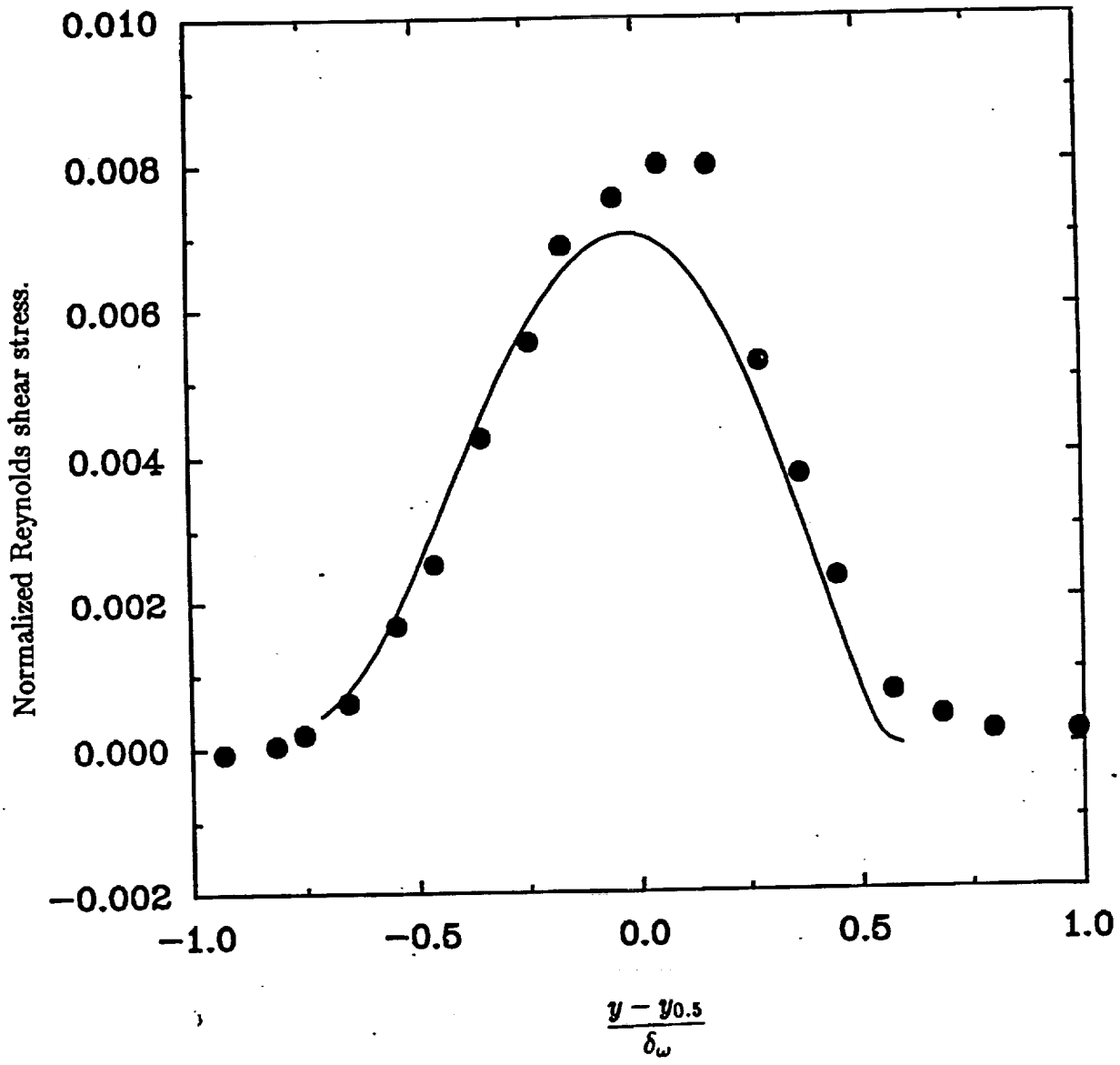

Figure 4. Comparison of Reynolds shear stress for the shear layer in Case 1 of Elliott and Samimy (1991). ——, Present; ● , experiment.

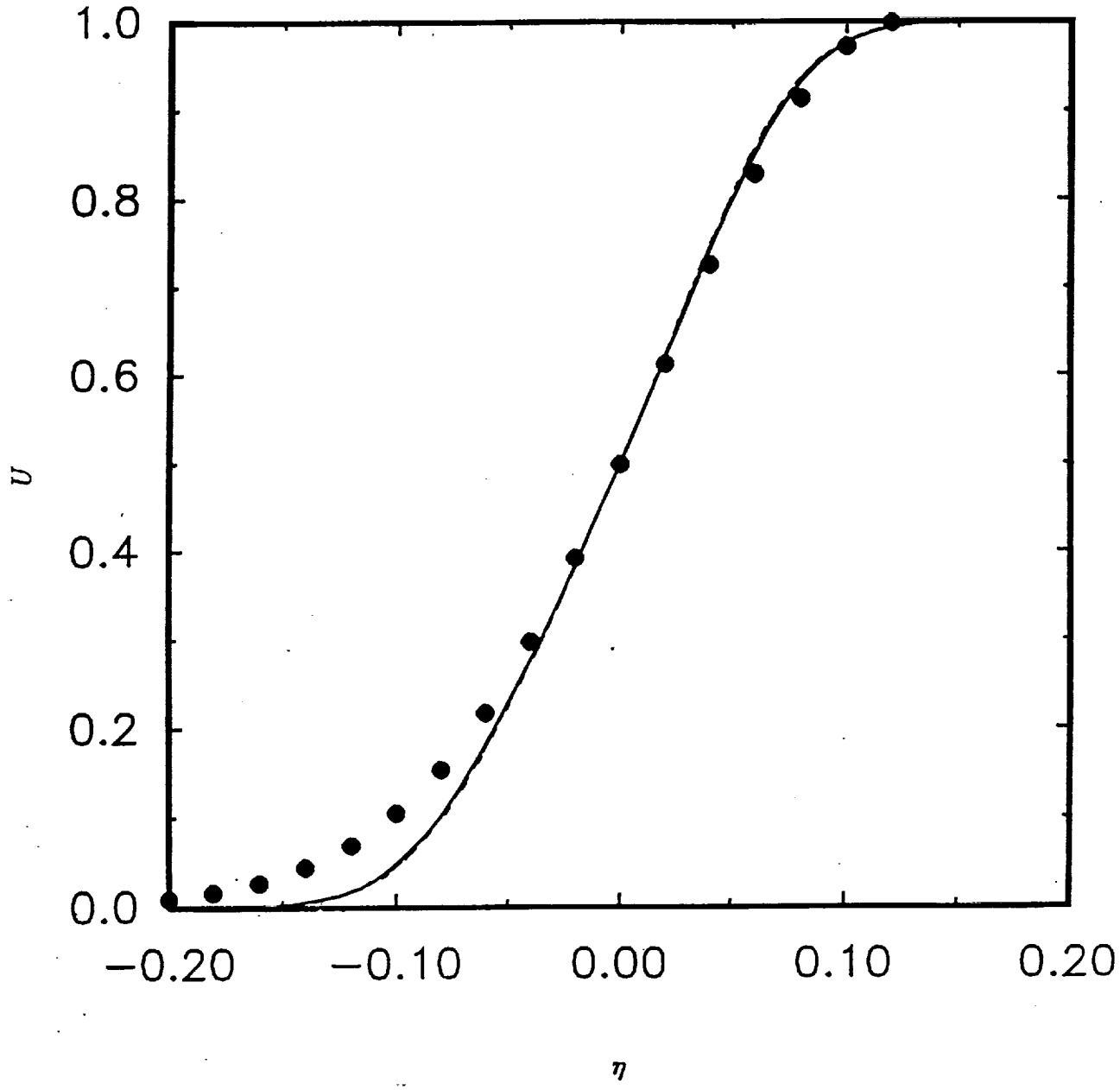

Figure 5. Mean velocity profiles. - - -, $x = 3.82$; - ——, 4.43; ——— , 5.99; • , Patel[9].

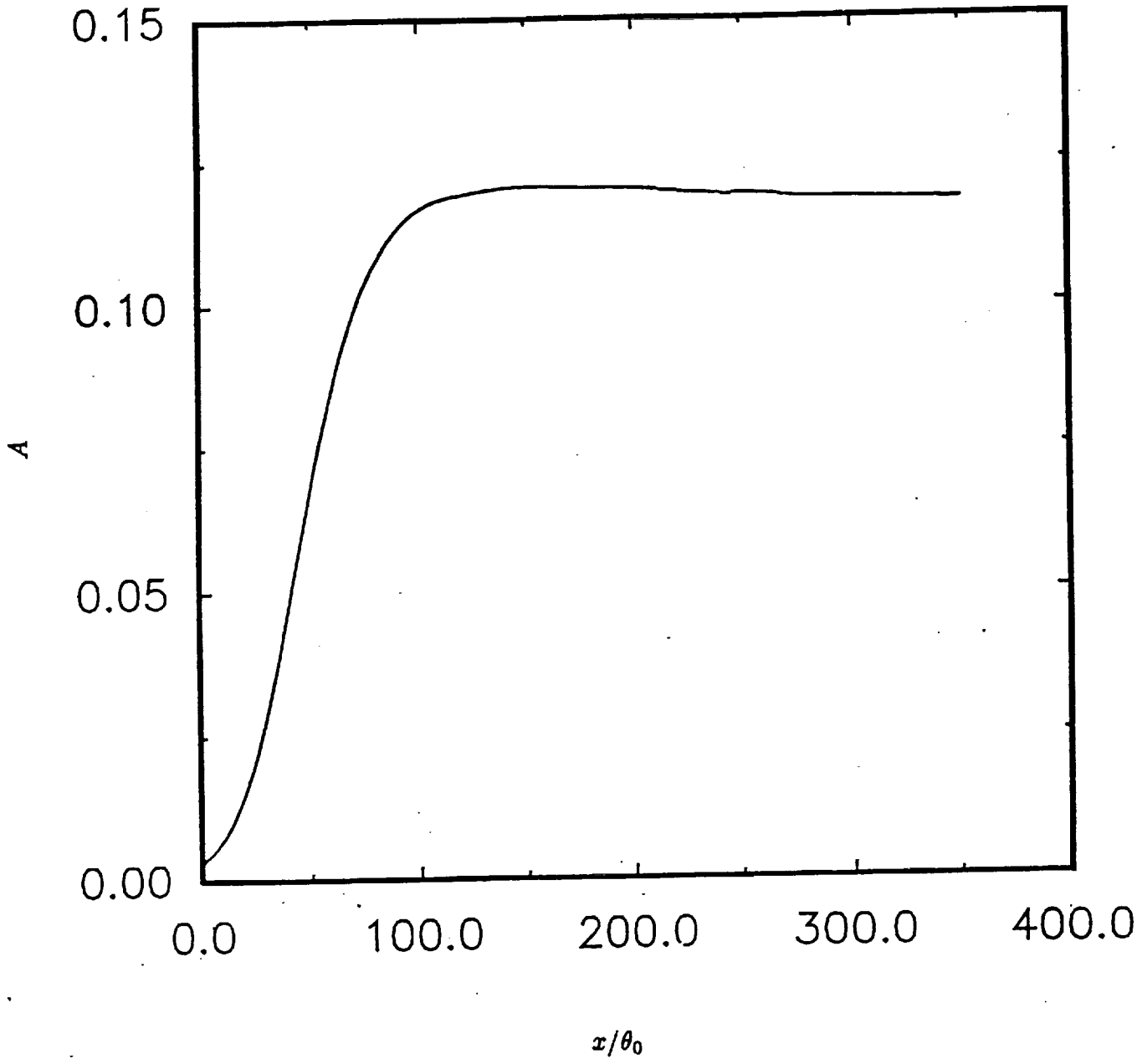

Figure 6. Variation of the wave amplitude with streamwise distance.